

January 2009

# A 32 kb 10T sub-threshold sram array with bit-interleaving and differential read scheme in 90 nm CMOS

Ik Joon Chang

Jae-Joon Kim

Sang Phill Park

Kaushik Roy

Follow this and additional works at: <http://docs.lib.purdue.edu/ecepubs>

---

Chang, Ik Joon; Kim, Jae-Joon; Park, Sang Phill; and Roy, Kaushik, "A 32 kb 10T sub-threshold sram array with bit-interleaving and differential read scheme in 90 nm CMOS" (2009). *Department of Electrical and Computer Engineering Faculty Publications*. Paper 8. <http://dx.doi.org/http://dx.doi.org/10.1109/JSSC.2008.2011972>

This document has been made available through Purdue e-Pubs, a service of the Purdue University Libraries. Please contact [epubs@purdue.edu](mailto:epubs@purdue.edu) for additional information.

# A 32 kb 10T Sub-Threshold SRAM Array With Bit-Interleaving and Differential Read Scheme in 90 nm CMOS

Ik Joon Chang, Jae-Joon Kim, Sang Phill Park, *Student Member, IEEE*, and Kaushik Roy, *Fellow, IEEE*

**Abstract**—Ultra-low voltage operation of memory cells has become a topic of much interest due to its applications in very low energy computing and communications. However, due to parameter variations in scaled technologies, stable operation of SRAMs is critical for the success of low-voltage SRAMs. It has been shown that conventional 6T SRAMs fail to achieve reliable subthreshold operation. Hence, researchers have considered different configuration SRAMs for subthreshold operations having single-ended 8T or 10T bit-cells for improved stability. While these bit-cells improve SRAM stability in subthreshold region significantly, the single-ended sensing methods suffer from reduced bit-line swing due to bit-line leakage noise. In addition, efficient bit-interleaving in column may not be possible and hence, the multiple-bit soft errors can be a real issue. In this paper, we propose a differential 10T bit-cell that effectively separates read and write operations, thereby achieving high cell stability. The proposed bit-cell also provides efficient bit-interleaving structure to achieve soft-error tolerance with conventional Error Correcting Codes (ECC). For read access, we employ dynamic DCVSL scheme to compensate bitline leakage noise, thereby improving bitline swing. To verify the proposed techniques, a 32 kb array of the proposed 10T bit-cell is fabricated in 90 nm CMOS technology. The hardware measurement results demonstrate that this bit-cell array successfully operates down to 160 mV. For leakage power comparison, we also fabricated 49 kb arrays of the 6T and the proposed 10T bit-cells. Measurement results show that the leakage power of the proposed bit-cell is close to that of the 6T (between 0.96x and 1.22x of 6T).

**Index Terms**—Low voltage SRAM design, robust subthreshold operation of SRAM, voltage scaling in SRAM.

## I. INTRODUCTION

**P**ORTABLE applications such as implantable medical devices and wireless sensor networks require ultra-low power dissipation. Many researchers have explored digital subthreshold logic [1], [2] as a possible option to deliver this requirement. The low voltage operation (below 400 mV) of such designs has been successfully demonstrated in real silicon measurements [2]. However, operating memory circuits at such a low voltage is more challenging since SRAM yield degrades

considerably at these low voltages. In the subthreshold region, conventional 6T SRAM experiences poor read stability or weak writability [3]. Since the read stability and the writability have conflicting design requirements, it is extremely difficult to operate the 6T SRAM in the subthreshold region. To overcome this problem, researchers have considered different configuration for SRAM cells. For example, [10] employed Schmitt-trigger based SRAM cell, enhancing read stability and writability simultaneously. To further increase read SNM, single-end 8T [4] or 10T [3], [5] SRAMs have been explored. In these schemes, data nodes are fully decoupled from read access. It ensures read SNM to be almost the same as hold SNM, improving read stability significantly. In addition, several design techniques such as supply power gating [3] and long-channel access transistors [5] also have been proposed for writability improvement. The subthreshold operation of the designs with these techniques has been verified through hardware measurement data as well [3], [5]. However, the single-end 8T or 10T SRAMs cannot efficiently deal with multiple bit soft-errors, which can have large impact on SRAM operation in the subthreshold region. As supply power ( $V_{DD}$ ) scales down, soft-error rate (SER) increases [7]. Moreover, in the subthreshold region, *critical charge* ( $Q_c$ ) [8] is also reduced due to low gate capacitance and hence, SER can be much larger than that in the superthreshold region. In conventional SRAMs, adjacent bits are implemented as different logic words. In this bit-interleaved structure, conventional Error Correction Code (ECC) can address multiple bit soft-errors easily [9]. On the other hand, due to pseudo-read problem [5], we may not obtain efficient bit-interleaving structure in the 8T and 10T subthreshold SRAMs [3], [4]. In addition, the single-end 8T and 10T SRAMs suffer from small bitline swing in subthreshold operation. To improve the bitline swing, a peripheral circuit called buffer-foot has been proposed [4]. This technique can mitigate the subthreshold leakage noise current from bitline. Nonetheless, other leakage components (e.g., junction leakage) still degrade the bitline swing significantly, incurring functional failures during read access. A virtual ground scheme has been proposed to utilize the small bitline swing more efficiently [5]. However, the raised virtual ground also reduces the sense margin of the following inverter buffer and hence, this scheme may not improve the sense margin effectively.

In this work, we propose a fully differential 10T subthreshold SRAM [6]. The contributions of this work can be summarized as follows:

- Our bit-cell provides isolation of read and write operations leading to improved noise margin.

Manuscript received April 06, 2008; revised November 11, 2008. Current version published January 27, 2009. The work of I. J. Chang, S. P. Park, and K. Roy was supported in part by Semiconductor Research Corporation and by a grant from Boeing Corporation.

I. J. Chang, S. P. Park, and K. Roy are with the School of Electrical and Computer Engineering, Purdue University, West Lafayette, IN 47907 USA (e-mail: ichang@purdue.edu; park143@purdue.edu; kaushik@purdue.edu).

J.-J. Kim is with the IBM T. J. Watson Research Center, Yorktown Heights, NY 10598 USA (e-mail: jjkim2@us.ibm.com).

Color versions of one or more of the figures in this paper are available online at <http://ieeexplore.ieee.org>.

Digital Object Identifier 10.1109/JSSC.2008.2011972

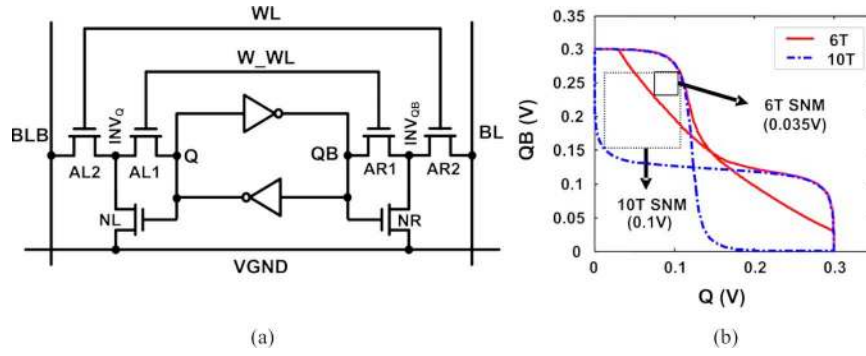


Fig. 1. (a) Our proposed 10T SRAM cell (b) SNM comparison of conventional 6T and our 10T cells.

- A column-by-column write control enables implementation of bit-interleaving structure efficiently. Therefore, soft-error tolerance can be achieved with conventional ECC.
- Dynamic Differential Cascade Voltage Switch Logic (DCVSL) scheme is employed for read access. In this scheme, bitline leakage noise is compensated by the drive current of a keeper, providing large bitline swing.
- During hold mode, subthreshold component of bitline leakage current is significantly reduced due to stacked bitline leakage path.

To verify the proposed technique, we fabricated the proposed bit-cell in 32 kb SRAM array in 90 nm CMOS. The measurement results show that our SRAM successfully operates below 300 mV  $V_{DD}$ .

## II. PROPOSED 10T SUBTHRESHOLD SRAM

### A. The Proposed 10T SRAM and Operating Principle

Fig. 1(a) shows our proposed 10T SRAM cell [6]. The operating principle of our 10T SRAM can be summarized as follows using the timing diagram in Fig. 2. In read mode, WL is enabled and VGND is forced to 0 V while W\_WL remains disabled. The disabled W\_WL makes data nodes ('Q' and 'QB') decoupled from bitline during the read access. Due to this isolation, the read SNM of our 10T cell is almost same as the hold SNM of conventional 6T cell. Since hold SNM is much larger than read SNM in the 6T cell, read stability is remarkably improved in our 10T cell (Fig. 1(b)). Depending on the cell data value, one of the bitlines starts discharging after WL is enabled. In our 10T cell, the read value is developed as an inverted signal of cell data and hence, we exchange the position of BL and BLB, as shown in Fig. 1(a).

During write mode, both WL and W\_WL are enabled to transfer the write data to cell node from bitlines. As discussed in the introduction, weak writability is another major challenge for subthreshold SRAMs. Since our 10T cell has series access transistors, writability is a critical issue. In some previous subthreshold SRAMs [3], [4],  $V_{DD}$  is collapsed to enhance writability, as shown in Fig. 3(a). However, it also degrades hold stability of the SRAM cells in other row sharing the  $V_{DD}$  line. To operate this technique successfully, each row should have individual  $V_{DD}$  line (Fig. 3(b)), resulting in large area penalty (more than 50% in thin-cell layout assuming poly pitch cannot

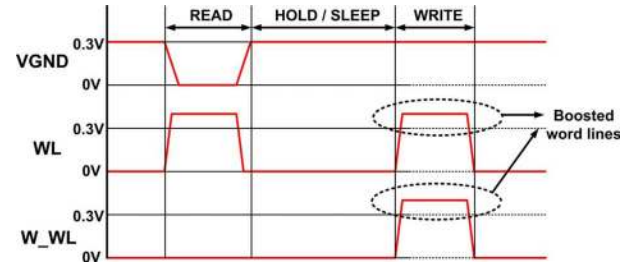


Fig. 2. This timing diagram explains the operating principle of our 10T SRAM.

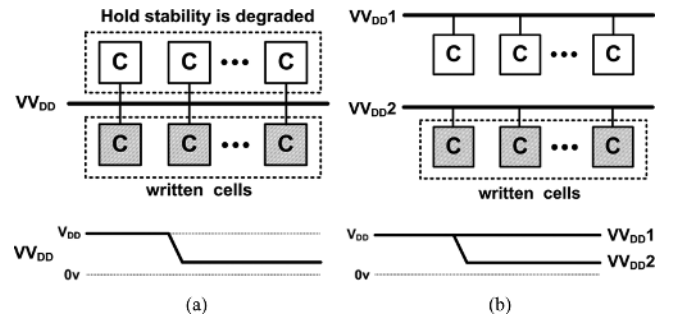


Fig. 3. (a) In the previous works [3], [4], supply power is collapsed for the write. It threatens the hold stability of other rows sharing the supply power line. (b) For the successful operation of the supply power collapsing, individual supply power line is required. But, this scheme incurs large area penalty.

be altered [11]). In this work, we boost  $V_{WL}$  and  $V_{W\_WL}$  by 100 mV (at 300 mV  $V_{DD}$ ) to compensate weak writability. Since the gate input boosting overwhelms sizing effect in the subthreshold region, we can obtain strong writability without incurring large area penalty in spite of having series access transistors. Fig. 4 shows that such boosting provides good writability even in the worst-case process corner (Slow NMOS and Fast PMOS).

In order to reduce the area overhead of a VGND driver, VGND node can be shared by several SRAM cells. In this work, four columns have a common VGND node, as shown in Fig. 5. Hence, we made the pull-down transistor of the VGND driver four times larger than the evaluation transistors of an SRAM cell (NL and NR in Fig. 1(a)). Note that the pull-down strength of the VGND driver can be weakened due to process variations, degrading read current significantly. To mitigate this effect, we employed dynamic-threshold MOS (DTMOS) technique for the VGND driver (Fig. 5). In this scheme, the

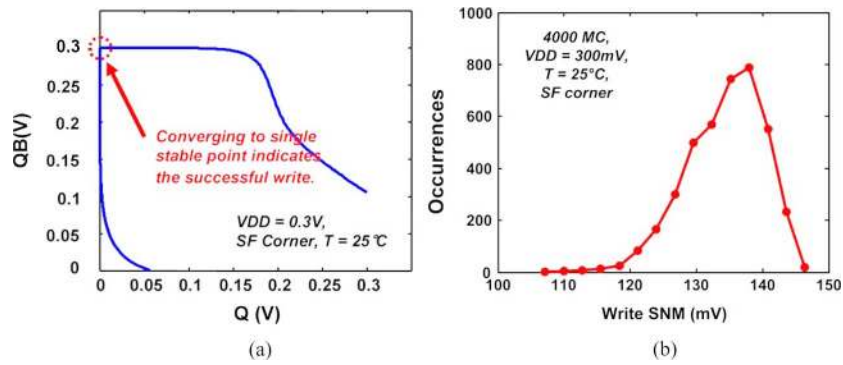


Fig. 4. (a) Voltage transfer characteristic curves of write mode at  $V_{DD} = 300$  mV. (b) Monte Carlo simulation results for the write margin (write SNM). For entire simulations,  $V_{WT}$ , and  $V_{W\_WT}$ , are boosted by 100 mV.

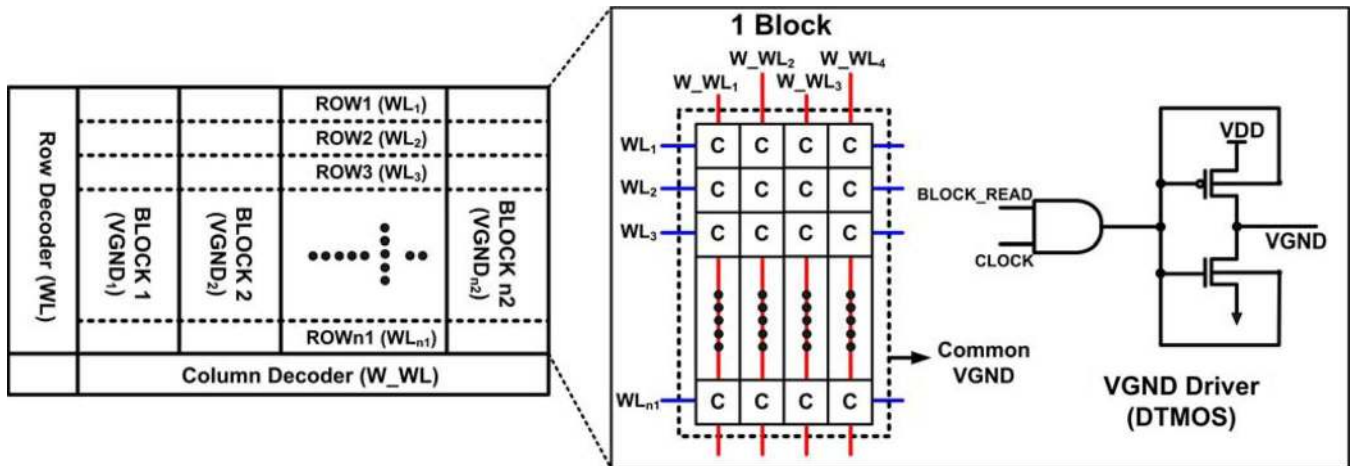


Fig. 5. SRAM Array architecture and a VGND driver.

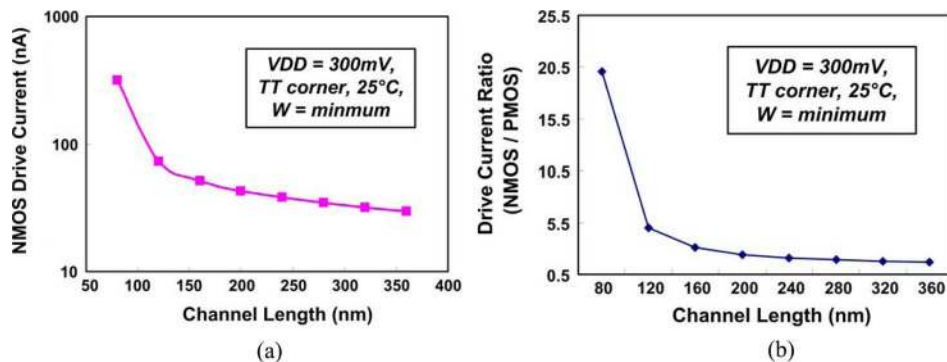


Fig. 6. Since NMOS shows extreme  $V_t$ -roll off [13] in 90 nm CMOS, pull-down of NMOS is much stronger than pull-up of PMOS in short-channel length region (a) Minimum width NMOS drive current in 90 nm CMOS (b) Drive current ratio between minimum width NMOS and PMOS.

pull-down device is forward-biased during read, enhancing the drive current. In superthreshold operation, the DTMOS technique may incur faulty operations due to forward biasing current of PN junction. Since our SRAM is designed for subthreshold operation (below 300 mV), the forward biasing current is not critical.

### B. Gate Length Modulation

In sub-100 nm technologies, threshold voltage ( $V_t$ ) varies significantly in small geometry transistors. Since transistor current is extremely sensitive to  $V_t$  variation in the subthreshold region and the small size transistors are employed in an SRAM cell,  $V_t$  variation may have larger impact on the stability of subthreshold SRAM compared to superthreshold SRAM. For example, NMOS transistors experience large  $V_t$  roll-off [13] in

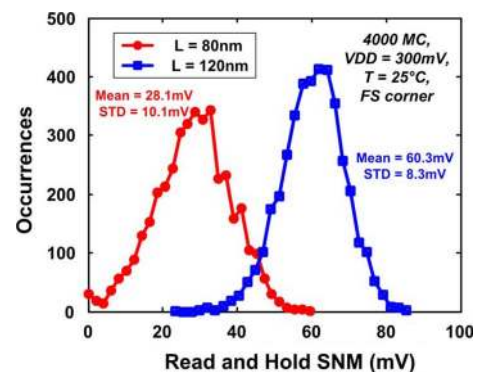


Fig. 7. Read (Hold) SNM simulation results ( $V_{DD} = 300$  mV,  $T = 25^\circ\text{C}$ ). The gate length modulation from 80 nm to 120 nm improves overall read (hold) SNM significantly.

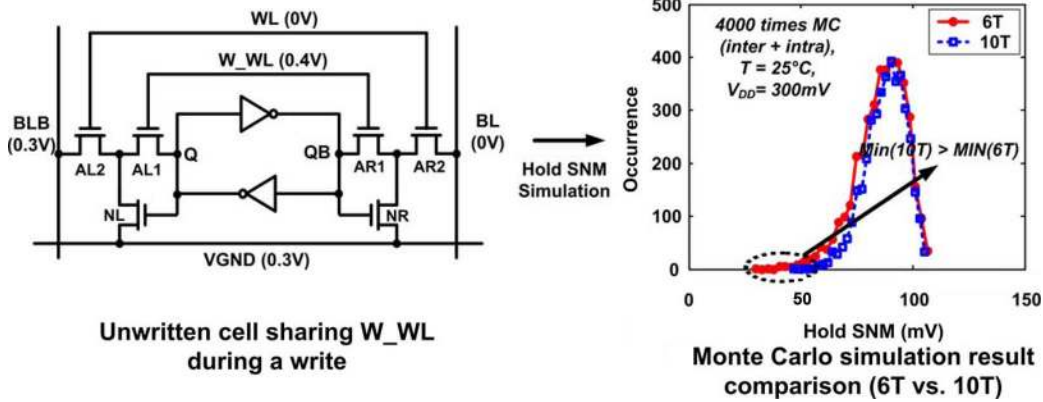


Fig. 8. For the cell sharing  $W\_WL$  with the written cell, Monte Carlo simulation shows that the hold stability is almost comparable to that of the conventional 6T cell.

short-channel length region of the technology which we use for this paper, as shown in Fig. 6(a). In this situation, pull-down transistor becomes much stronger than pull-up transistor at short-channel lengths (Fig. 6(b)). In addition, the short-channel  $V_t$  roll-off makes transistor current more sensitive to other parameter variations such as line-edge roughness [14]. These effects degrade read and hold stability of SRAM considerably. To mitigate this problem, we need to modulate transistor gate length. Since the variation of drive current ratio between NMOS and PMOS starts to stabilize around 120 nm gate length (Fig. 6(b)), we employ 120 nm length for the pull-up PMOS's and pull-down NMOS's in the proposed SRAM cell. The effectiveness of this gate length modulation can be verified through Monte Carlo (MC) simulation. The Fig. 7 shows 4000 Monte-Carlo (MC) simulation results for the read (hold) SNM of two different gate length 10T SRAM cells at fast NMOS and slow PMOS corner, which is the worst-case process corner for read and hold stability. Compared to the cell with the minimum channel length transistors, the cell with 120 nm channel length transistors provides 114.6% improvement in the mean value of read (hold) SNM.

### III. EFFICIENT BIT-INTERLEAVING FOR SOFT-ERROR IMMUNITY

According to [7], SER increases by 18% for every 10%  $V_{DD}$  reduction and hence, SER in 0.3 V  $V_{DD}$  can be 8.6X higher than that in 1.2 V  $V_{DD}$ . Low gate capacitance of weak inversion makes the problem worse due to the reduction of *critical charge* ( $Q_c$ ) [8]. Hence, it is clear that soft-error is more critical in subthreshold SRAMs compared to its superthreshold counterpart. A soft-error may flip adjacent multiple bits simultaneously [9]. In conventional SRAMs, multiple bit soft-errors can be corrected by bit-interleaving and ECC [9]. In the bit-interleaving structure, multiple bit errors are regarded as single bit errors of several logic words. Since conventional ECC techniques can detect and correct single bit errors, bit-interleaving enables us to handle multiple bit soft-errors efficiently.

Bit-interleaving structure may not be efficiently applicable in the previous subthreshold SRAMs [3]–[5]. For these SRAMs, other cells sharing a word line suffer from pseudo-read problem [5] while writing into a cell, degrading their hold stability significantly. To avoid this problem, the entire cells sharing a word line

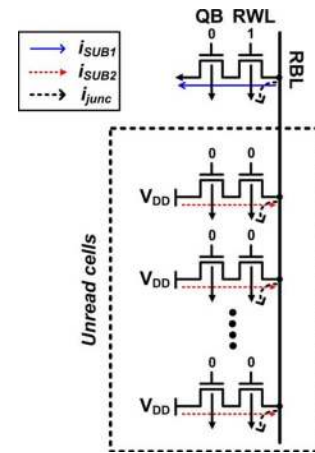


Fig. 9. The worst-case data pattern of the single-end 8T SRAM [4].

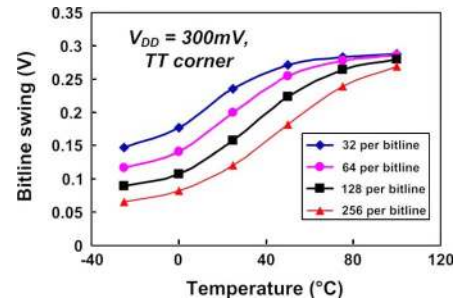


Fig. 10. Bitline swing simulation results of Fig. 9 ( $V_{DD} = 300$  mV, typical process corner) We measured the bitline swing at steady-state after RWL turns on.

are written at the same time in [3], [4]. In such a scenario, adjacent bits need to be implemented as the same logic word, making the SRAMs exposed to multiple bit soft-errors. [5] employs a *write after read* scheme for bit-interleaving. However, in this scheme, extra read operation is required for a write. It should also be noted that due to full-swing read, the read operation consumes comparable power to the write in one column. If we consider the read power of unselected columns, this scheme increases total write power dissipation. In addition, overall write delay increases since additional read operation is needed before write.

On the other hand, writing a cell hardly affects the hold stability of other cells in the proposed 10T SRAM [6]. As shown

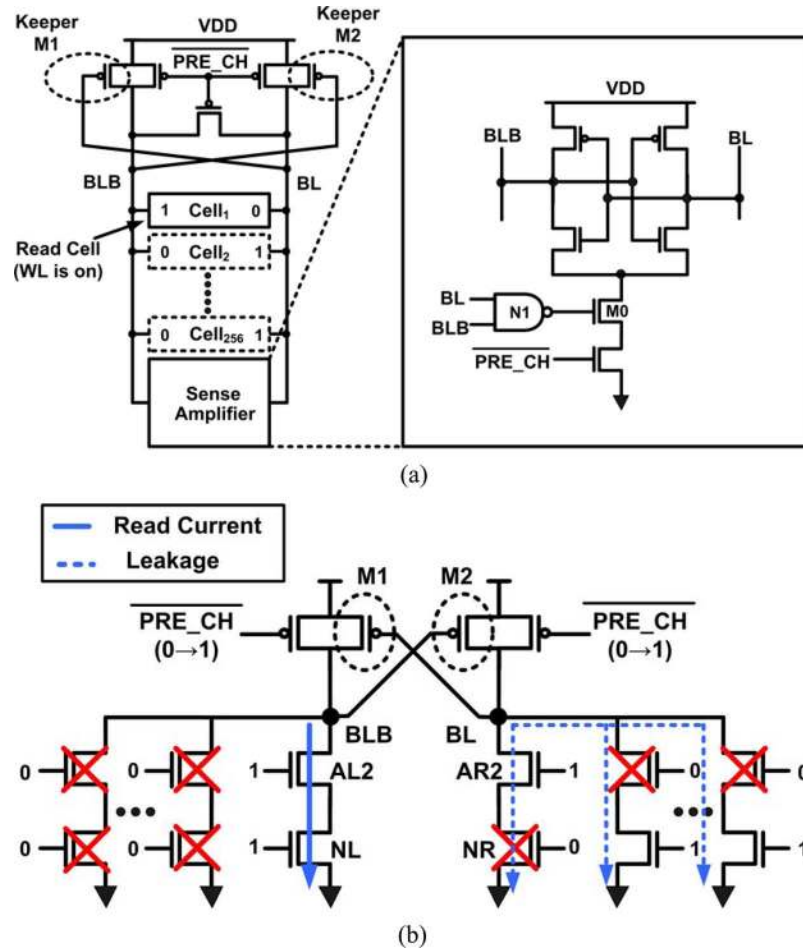


Fig. 11. (a) Column architecture of our SRAM (b) The figure of (a) is unfolded equivalently. In our SRAM, dynamic DCVSL read scheme is used for the read sensing. The data input pattern shows the worst-case leakage scenario of our SRAM.

in Fig. 5,  $W\_WL$  is shared by the cells in a column. When the  $W\_WL$  of a column is raised for writing a cell,  $W\_WL$ s of other columns are still maintained at 0 V. Hence, the rise of  $WL$  does not influence hold stability of unwritten cells sharing the  $WL$ . MC simulation results in Fig. 8 indicate that the hold stability of unwritten cells sharing  $W\_WL$  does not degrade during write as well. As shown in this figure, mean hold SNM of these cells has 2.4% improvement compared to that of conventional 6T cell. Moreover, the minimum hold SNM, which is more critical in SRAM design, is improved by 59%. It is because the drive current flowing through NMOS transistors (NL and NR) from VGND node compensates weak pull-up current at fast NMOS and slow PMOS corner, which is the worst-case process corner for hold stability. Since the hold stability of adjacent cells is not affected during a write, bit-interleaving can be implemented efficiently in our design, thereby achieving soft-error immunity with conventional ECC.

#### IV. DIFFERENTIAL READ SCHEME

##### A. Sense Margin Problem in Single-Ended Read Schemes

In [3]–[5], single-ended read scheme has been used. Since such a scheme relies on the trip voltage of an inverter or an absolute reference voltage, their sense margin is at most  $0.5 V_{DD}$ . Considering undefined region of inverter or offset voltage of

sense amplifier, effective sense margin can be much smaller. Moreover, due to slow speed and small  $I_{on} - I_{off}$  ratio in subthreshold operation, bitline leakage noise reduces bitline swing considerably, further deteriorating the sense margin.

To mitigate the bitline leakage noise, several approaches have been explored in [3]–[5]. For example, buffer-foot scheme is employed in [4] to increase bitline swing. Fig. 9 shows the worst-case data pattern for the bitline swing in this scheme. Since ‘QB’ of the accessed cell is ‘0’, RBL should not be discharged. However, subthreshold leakage noise ( $i_{SUB1}$ ) and junction leakage noise ( $i_{junc}$ ) discharge RBL significantly. Although other subthreshold leakage current ( $i_{SUB2}$ ) compensates for the discharging, the ‘ $i_{SUB2}$ ’ decreases exponentially due to stacked leakage paths of this data input pattern. We simulated this scenario in a 90 nm CMOS technology. The graph of Fig. 10 shows the simulation results of the bitline swing, which are measured at steady-state after RWL turns on. In low temperature region, junction leakage noise ( $i_{junc}$ ) is much larger than the ‘ $i_{SUB2}$ ’ and hence, bitline swing degrades considerably (below  $0.5 V_{DD}$  at 32 cells per bitline). At the worse-case process corner, the bitline swing is expected to be further deteriorated. These make it difficult to distinguish logic high and low from the developed bitline swing and hence, we believe that a differential read scheme is more appropriate for subthreshold operation.

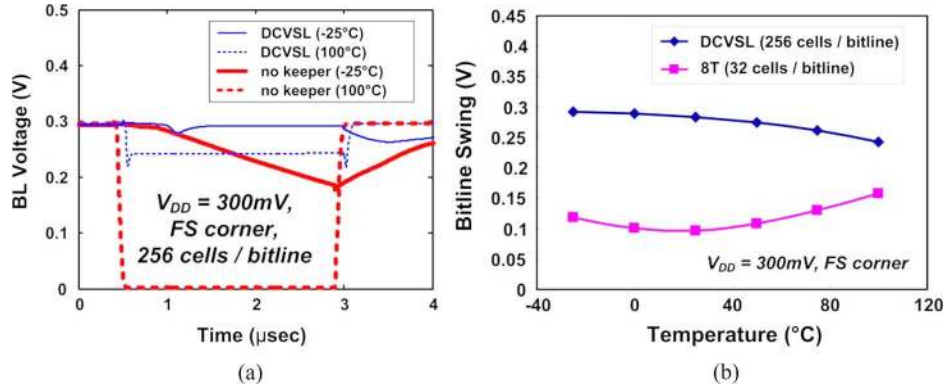


Fig. 12. (a) Transient simulation results for Fig. 11(b). We compare the results with the simulation results of other design, which do not have the keeper M1 and M2. (b) Comparison of the bitline swing simulation results between our 10T SRAM and the single-end 8T [4]. For two designs, we used the worst-case leakage scenario (Figs. 10, 11) and the worst-case process corner (Fast NMOS and Slow PMOS).

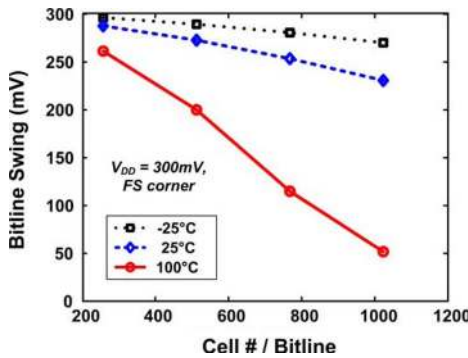


Fig. 13. Final bitline swing simulation results of our 10T SRAM. For these simulations, we include a sense amplifier in the design.

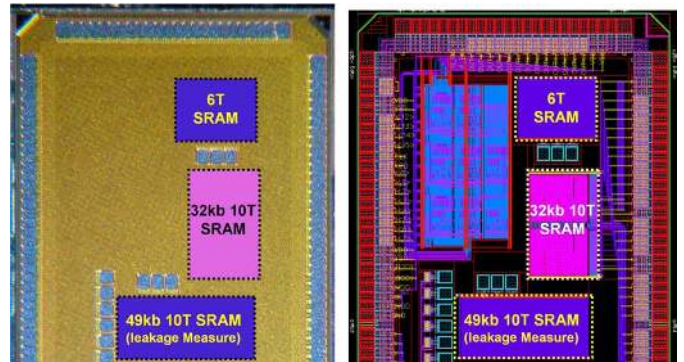


Fig. 14. Die micrograph and layout.

**B. Dynamic DCVSL Read Scheme**

The proposed SRAM has a fully differential read scheme, which improves the bitline noise immunity during read. The column structure of Fig. 11(a) explains our read mechanism. When read begins, the word lines (WL and W\_WL) of the accessed SRAM cells are raised and precharge signal (PRE\_CH) is disabled. Depending on the data value of the access cell, one of the precharged bitlines (BL or BLB) starts discharging. The unfolded circuit diagram of Fig. 11(b), which is equivalent to the column of Fig. 11(a), shows the worst-case data pattern for bitline leakage noise. During read, the leakage current through unselected cells (storing complementary value in the accessed cell) impedes a successful read operation. To obtain the leakage tolerance, we employ dynamic DCVSL technique. In this technique, the discharge of BLB turns on keeper M2 and hence, bitline leakage current in BL is compensated by the drive current of M2.

Transient simulation results of Fig. 12(a) verify the effectiveness of the dynamic DCVSL read scheme. Without any keeper, BL node is considerably discharged at Fast NMOS and Slow PMOS (FS) process corner. However, in the dynamic DCVSL scheme, the keeper drive current prevents discharging, providing large differential bitline swing ( $0.8 V_{DD}$ ). We compare the bitline swing to that of the single-end 8T SRAM [4]. For the 8T SRAM, we set up 32 cells per each bitline. In spite of larger number of cells per bitline (256 cells/bitline), DCVSL read provides much bigger bitline swing than the single-ended read of 8T SRAM, as shown in Fig. 12(b).

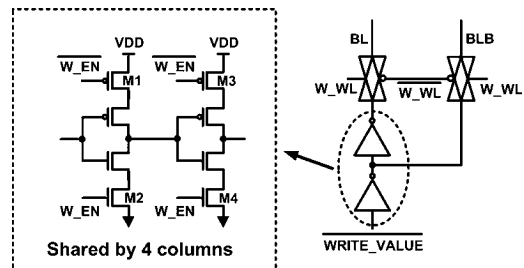


Fig. 15. The write driver in the test-chip. Four columns share one write driver. Since the position of BL and BLB is exchanged, the write data is inverted for the correct writing.

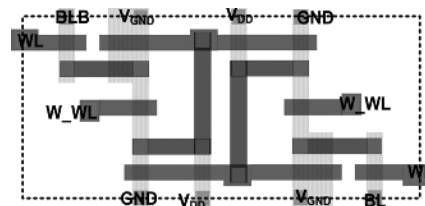


Fig. 16. Thin-cell layout of our 10T bit-cell. Compared to the 8T bit-cell, the area penalty is 61%.

In order to further improve the bitline leakage tolerance, we add sense amplifier using cross-coupled inverters. In the sub-threshold region, intra-die variation results in large delay variation and increases the worst-case offset voltage of the sense amplifier. Hence, extremely long delay buffer is required for strobe timing [12], incurring large area and performance penalty. In this work, we employ the footer transistor M0 instead of the strobe-delay method (Fig. 11(a)). Drive current flowing through

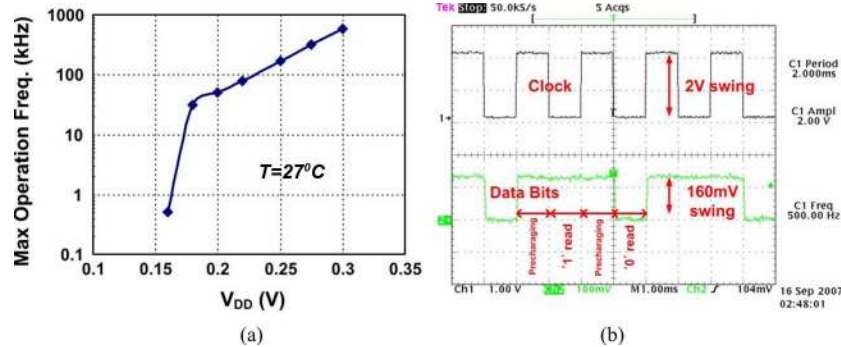


Fig. 17. (a) Measured maximum operating frequency. The word line drivers are boosted by 33% of  $V_{DD}$ . Below 180 mV, more aggressive boosting is required. (b) Measured waveforms ( $V_{DD} = 160$  mV, 80 mV word line boosting).

M0 is almost negligible before there is significant discharging from a bitline, preventing malfunction induced by the offset voltage of the sense amplifier. Fig. 13 shows the simulation results of the bitline swing when the sense amplifier is included. In spite of extreme temperature variations ( $-25^{\circ}\text{C} \sim 100^{\circ}\text{C}$ ), 0.68  $V_{DD}$  bitline swing develops for 512 cells per bitline at the worst-case process corner (Fast NMOS and Slow PMOS).

## V. TEST-CHIP IMPLEMENTATION AND MEASUREMENT RESULT

### A. Test-Chip Implementation

To verify the proposed SRAM, we fabricated test-chips in 90 nm, 8-metal CMOS technology. Fig. 14 shows the die micrograph and layout of the test-chip. For performance and power measurement, a 32 kb SRAM array is implemented using our cell as shown in Fig. 14. The SRAM array has 256 rows and 192 columns, which are divided into 24 sub-blocks (8 columns per a sub-block). Each sub-block has two VGND and write drivers. Leakage current through the write driver reduces bitline swing, and hence stacked transistors are used to reduce this leakage as shown in Fig. 15. Since a boosted signal is used for  $W\_WL$  and  $W\_EN$ , degradation of writability resulting from IR-drop of the stacked NMOS structure in the write driver is almost negligible. As discussed in Section II-A, the position of BL and BLB is exchanged in our SRAM and hence, the write data is also inverted for correct writing as shown in this figure. To generate input and clock signals, we used a Tetronix pattern generator. Since this equipment has 2 V output swing, we down-converted the voltage for the input and clock signals using level-down converters. To obtain boosting effect in the word line drivers, we separated power supply pad for row and column decoders from that of other parts. For leakage comparison, 49 kb SRAM arrays are implemented for both conventional 6T cell and our 10T cell. Only cell arrays and VGND driver are implemented in these arrays. We employ direct probe pad for supply power of these arrays to exclude leakage current through ESD diode in the I/O pad.

The layout of our SRAM is shown in Fig. 16. In the schematic of Fig. 1(a), the node 'INV<sub>Q</sub>' and 'INV<sub>QB</sub>' cannot be shared by other adjacent cells. Hence, we need at least 3 poly pitches for the thin-cell layout [11] of our SRAM cell. Due to this characteristic of thin-cell layout, our 10T SRAM adds 61% area overhead relative to 8T SRAM of [4]. However, the overall area penalty

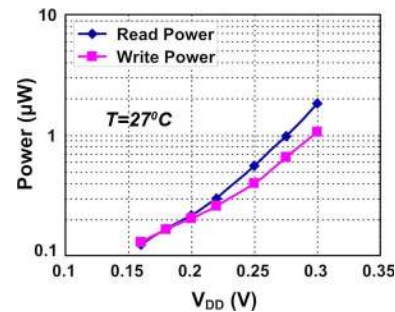


Fig. 18. Measured read and write power dissipation.

is less since we can include more cells on the bitline (explained in Section IV-B).

### B. Performance and Power Measurement

In the power and performance measurement, we assumed that  $V_{DD}$  of word line drivers is boosted by 33% of the SRAM array  $V_{DD}$ . The environment temperature is set to  $27^{\circ}\text{C}$  during measurement. Fig. 17(a) shows the maximum operation frequency, which is measured with the 33% boosting of word line drivers. At 300 mV  $V_{DD}$ , our SRAM functions correctly at 581.4 kHz clock frequency. The frequency decreases exponentially due to the subthreshold MOS device characteristic as the  $V_{DD}$  scales down. The minimum  $V_{DD}$  for successful read operation was 160 mV. The measured waveforms at this voltage are shown in Fig. 17(b). As discussed earlier, 2 V input and clock signal is leveled down inside the test-chip. To verify the read operation, we wrote complementary data between adjacent cells and read them sequentially. The output signal toggles per 2 clock cycles, which successfully demonstrates 500 Hz read operation at 160 mV  $V_{DD}$ . For the write operation, the minimum  $V_{DD}$  was 180 mV. However, we can further scale down the  $V_{DD}$  to 160 mV with more aggressive word line boosting (50% boosting for  $V_{DD}$ ).

We measured total read and write power dissipation for the maximum operation frequency, which is shown in Fig. 18. At 300 mV  $V_{DD}$ , our design dissipates 1.81  $\mu\text{W}$  and 1.07  $\mu\text{W}$  power for read and write, respectively. Interestingly, the read power dissipation is larger than the write power, which is due to full-swing read method. Moreover, VGND nodes are also switched for the read, incurring more power dissipation.



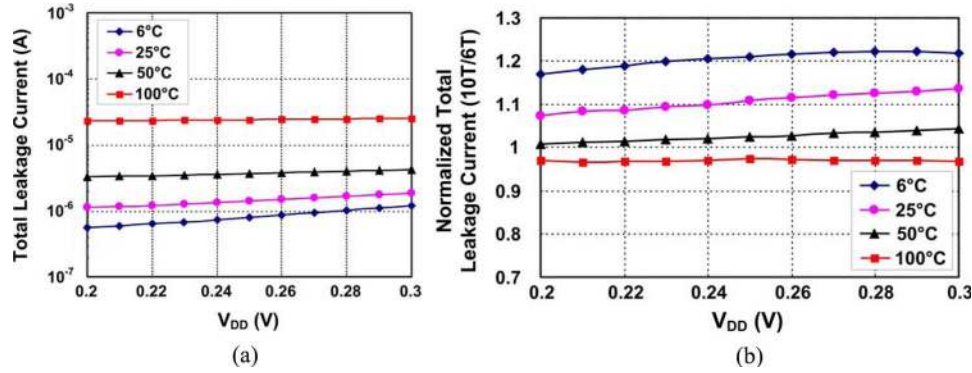


Fig. 19. (a) Leakage measurement results of our 10T SRAM (b) Leakage measurement result comparison of our 10T and the 6T.

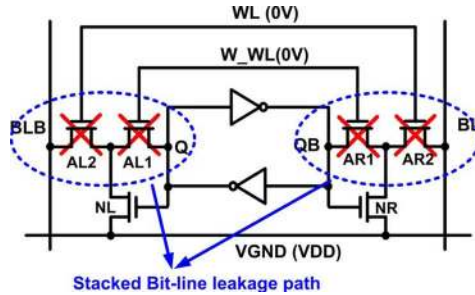


Fig. 20. In our 10T bit-cell, the bitline leakage paths have stacked devices, reducing subthreshold leakage from the bitlines to cell node.

### C. Leakage Measurement

Leakage measurement results of the 49 kb arrays are summarized in Fig. 19. For these measurements, we swept the  $V_{DD}$  from 200 mV to 300 mV at different temperatures—6°C, 25°C, 50°C and 100°C. At 6°C and 300 mV  $V_{DD}$ , the total leakage current of the 10T SRAM is 1.21  $\mu$ A. As the temperature is raised, this leakage current increases exponentially as shown in Fig. 19(a). The graph of Fig. 19(b) shows the leakage comparison results between conventional 6T and our 10T SRAM. Due to extra cell transistors and VGND drivers, our SRAM has more junction and gate leakage compared to the 6T. Nonetheless, the total leakage current of our SRAM is close to that of the 6T (between 0.96x and 1.22x). This is due to the reduction of the bitline leakage. In our SRAM, the VGND node is forced to  $V_{DD}$  during the hold mode. In this situation, the leakage paths from the bitlines to the cell node have the stacked devices as shown in Fig. 20, reducing the subthreshold component of the bitline leakage drastically. This effort is more effective in high temperature region, as shown in Fig. 19(b). In the low temperature region, junction and gate leakages have profound impact on the total leakage current and hence, our SRAM still has the larger leakage current than the 6T cell. However, subthreshold leakage becomes dominant compared to other leakages at higher temperature. Hence, we observe that the total leakage current is almost comparable to that of the 6T beyond 50°C.

## VI. CONCLUSION

We propose a new differential 10T SRAM cell for the reliable subthreshold operation. Our main focus is enabling bit interleaving along the word line as well as designing reliable data read path. Previous subthreshold SRAM cells [3]–[5] used

single-ended read paths. The methods, however, suffer from reduced bitline swing due to bitline noise. In addition, the previous schemes need improvements in the bit-interleaving structure, which is critical to cope with multiple bit soft-errors. Our proposed 10T SRAM cell allows the bit interleaving with the column-wise write access control while having differential read path. To improve the read margin even further, we employ dynamic DCVSL read scheme. It allows large bitline swing despite of extreme process and temperature variations. Measurements of 32 kb 90 nm CMOS test-chip demonstrate successful operation of our 10T cell below 300 mV  $V_{DD}$ . The design operates at 31.25 kHz with 180 mV supply and 33% boosted WL and W-WL. With more aggressive word line boosting of 80 mV,  $V_{DD}$  can be scaled down to 160 mV. At this voltage, the operating frequency is 500 Hz and the read power dissipation is 0.123  $\mu$ W. We also implemented 49 kb arrays of 6T and the 10T cell for leakage comparison. The measurement results show that the leakage power consumption of our 10T SRAM is comparable to that of the 6T cell. It is due to the fact that our 10T cell has stacked bitline leakage paths and hence, the subthreshold component of bitline leakage current decreases significantly. Since the leakage power is substantial portion of total power in subthreshold logic, leakage reduction provides substantial total power saving.

## REFERENCES

- [1] H. Soeleman and K. Roy, "Ultra-low power digital subthreshold logic circuits," in *Int. Proc. Symp. Low Power Electronics and Design (ISLPED)*, 1999, pp. 94–96.
- [2] M. Hwang *et al.*, "A 85 mV 40 nW process-tolerant sub-threshold  $8 \times 8$  FIR filter in 130 nm technology," in *Symp. VLSI Circuits Dig.*, Jun. 2007, pp. 154–155.
- [3] B. H. Calhoun and A. Chandrakasan, "A 256 kb sub-threshold SRAM in 65 nm CMOS," *IEEE J. Solid-State Circuits*, vol. 42, no. 3, pp. 680–688, Mar. 2007.
- [4] N. Verma and A. Chandrakasan, "A 256 kb 65 nm 8T sub-Vt SRAM employing sense-amplifier redundancy," *IEEE J. Solid-State Circuits*, vol. 43, no. 1, pp. 141–149, Jan. 2008.
- [5] T. Kim, J. Liu, J. Keane, and C. H. Kim, "A high-density subthreshold SRAM with data-independent bitline leakage and virtual ground replica scheme," *IEEE J. Solid-State Circuits*, vol. 43, no. 2, pp. 518–529, Feb. 2008.
- [6] I. J. Chang, J. Kim, S. P. Park, and K. Roy, "A 32 kb 10T subthreshold SRAM array with bit-interleaving and differential read scheme in 90 nm CMOS," in *IEEE ISSCC Dig. Tech. Papers*, Feb. 2008, pp. 388–389.
- [7] P. Hazucha *et al.*, "Neutron soft error rate measurements in 90-nm CMOS process and scaling trends from 0.25- $\mu$ m to 90-nm generation," in *IEDM Tech. Dig.*, Dec. 2003, pp. 21.5.1–21.5.4.
- [8] C. Lage *et al.*, "Soft error rate and stored charge requirement in advanced high-density SRAMs," in *IEDM Tech. Dig.*, Dec. 1993, pp. 33.4.1–33.4.4.

- [9] J. Maiz, S. Hareland, K. Zhang, and P. Armstrong, "Characterization of multi-bit soft error events in advanced SRAMs," in *IEDM Tech. Dig.*, Dec. 2003, pp. 21.4.1–21.4.4.
- [10] J. Kulkarni, K. Kim, and K. Roy, "A 160 mV robust Schmitt trigger based sub-threshold SRAM," *IEEE J. Solid-State Circuits*, vol. 42, no. 10, pp. 2303–2313, Oct. 2007.
- [11] K. Nii *et al.*, "A 90 nm dual-port SRAM with 2.04 /spl mu/m/sup 2/ 8T-thin cell using dynamically-controlled column bias scheme," in *IEEE ISSCC Dig. Tech. Papers*, Feb. 2004, pp. 508–543.
- [12] K. Sohn *et al.*, "An autonomous SRAM with on-chip sensors in an 80 nm double stacked cell technology," in *Symp. VLSI Circuits Dig.*, Jun. 2005, pp. 232–235.
- [13] Y. Taur and T. Ning, *Fundamentals of Modern VLSI Devices*. New York: Cambridge Univ. Press, 2002.
- [14] A. Asenov, S. Kaya, and A. R. Brown, "Intrinsic parameter fluctuations in decananometer MOSFETs introduced by gate line edge roughness," *IEEE Trans. Electron Devices*, vol. 50, pp. 1254–1260, May 2003.

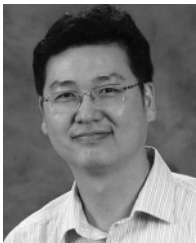


**Ik Joon Chang** received the B.S. degree in electrical engineering (*summa cum laude*) from Seoul National University, Seoul, Korea, and the M.S. degree from the School of Electrical and Computer Engineering, Purdue University, West Lafayette, IN, in 2002 and 2005, respectively. Since 2005, he has been pursuing the Ph.D. degree at Purdue University.

He worked with LG Electronics as a software engineer in 2003. During summer and fall of 2007, he had an internship with Qualcomm, CA, where he performed research related to low-power circuit tech-

niques. His current research interest is robust and low power circuit design in nanoscaled CMOS technologies.

Mr. Chang was awarded from the Samsung Scholarship Foundation in 2005.



**Jae-Joon Kim** received the B.S. and M.S. degrees in electronics engineering from Seoul National University, Seoul, Korea, and the Ph.D. degree from the School of Electrical and Computer Engineering, Purdue University, West Lafayette, IN, in 1994, 1998, and 2004, respectively.

He was with TLI Inc. Korea as a custom circuit designer from 1998 to 1999. During the summer of 2000, he was an intern at Intel Circuit Research Laboratory, Hillsboro, OR. He also spent the summer of 2001 and 2002 at IBM T. J. Watson Research Center,

Yorktown Heights, NY, for SOI circuit research. He has been with IBM T. J. Watson Research Center as a Research Staff Member since May 2004. His current research interest includes technology/circuit codesign.



**Sang Phill Park** (S'07) received the B.S. degree in computer engineering from University of Arizona, Tucson, AZ, in 2004. He is currently working toward the Ph.D. degree in electrical engineering at Purdue University, West Lafayette, IN.

In summer of 2008, he was with the Exploratory VLSI design group at IBM Austin Research Laboratory as an intern. His research interests include variation-tolerant circuit design and ultra-low power circuit design.



**Kaushik Roy** (SM'95–F'01) received the B.Tech. degree in electronics and electrical communications engineering from the Indian Institute of Technology, Kharagpur, India, and the Ph.D. degree in electrical and computer engineering from the University of Illinois at Urbana-Champaign in 1990.

He was with the Semiconductor Process and Design Center of Texas Instruments, Dallas, TX, where he worked on FPGA architecture development and low-power circuit design. He joined the electrical and computer engineering faculty at Purdue University, West Lafayette, IN, in 1993, where he is currently a Professor and holds the Roscoe H. George Chair of Electrical and Computer Engineering. His research interests include VLSI design/CAD for nanoscale silicon and non-silicon technologies, low-power electronics for portable computing and wireless communications, VLSI testing and verification, and reconfigurable computing. He has published more than 450 papers in refereed journals and conferences, holds eight patents, and is a coauthor of two books on low power CMOS VLSI design.

Dr. Roy received the National Science Foundation Career Development Award in 1995, IBM Faculty Partnership Award, ATT/Lucent Foundation Award, 2005 SRC Technical Excellence Award, SRC Inventors Award, Purdue College of Engineering Research Excellence Award, and Best Paper Awards at 1997 International Test Conference, IEEE 2000 International Symposium on Quality of IC Design, 2003 IEEE Latin American Test Workshop, 2003 IEEE Nano, 2004 IEEE International Conference on Computer Design, 2006 IEEE/ACM International Symposium on Low Power Electronics & Design, and 2005 IEEE Circuits and Systems Society Outstanding Young Author Award (Chris Kim), and 2006 IEEE TRANSACTIONS ON VLSI SYSTEMS Best Paper Award. He is a Purdue University Faculty Scholar. He was a Research Visionary Board Member of Motorola Labs (2002). He has been on the editorial board of *IEEE Design and Test*, IEEE TRANSACTIONS ON CIRCUITS AND SYSTEMS, and IEEE TRANSACTIONS ON VLSI SYSTEMS. He was Guest Editor for the Special Issue on Low-Power VLSI in the *IEEE Design and Test* (1994) and IEEE TRANSACTIONS ON VLSI SYSTEMS (June 2000), *IEEE Proceedings—Computers and Digital Techniques* (July 2002).